

Effect of magnetic field on the optical and thermodynamic properties of a high-temperature hadron resonance gas with van der Waals interactions

Bhagyarathi Sahoo, Kshitish Kumar Pradhan, Dushmanta Sahu, and Raghunath Sahoo*

Department of Physics, Indian Institute of Technology Indore, Simrol, Indore 453552, India

(Dated: June 7, 2023)

We study the behavior of a hadronic matter in the presence of an external magnetic field within the van der Waals hadron resonance gas (VDWHRG) model, considering both attractive and repulsive interactions among the hadrons. Various thermodynamic quantities like pressure (P), energy density (ϵ), magnetization (\mathcal{M}), entropy density (s), squared speed of sound (c_s^2), specific heat capacity at constant volume (c_v) are calculated as functions of temperature (T) and static finite magnetic field (eB). We also consider the effect of baryochemical potential (μ_B) on the above-mentioned thermodynamic observables in the presence of a magnetic field. Further, we estimate the magnetic susceptibility (χ_M^2), relative permeability (μ_r), and electrical susceptibility (χ_Q^2) which can help us to understand the system better. With the information of μ_r and dielectric constant (ϵ_r), we enumerate the refractive index (RI) of the system under consideration. Through this model, we quantify a liquid-gas phase transition in the T-eB- μ_B phase space.

PACS numbers:

I. INTRODUCTION

In the early stages of the evolution of the universe, it was supposed to be extremely hot and dense, possibly filled with a unique state of matter called Quark-Gluon Plasma (QGP). We explore the ultra-relativistic heavy-ion collisions in laboratories to probe such initial conditions. At extreme temperatures and/or baryon densities, the hadronic degrees of freedom transform into partonic degrees of freedom, resulting in QGP formation. Quantum-Chromodynamics (QCD) is the widely used theory to describe the behavior of QGP. In addition, studying its thermodynamic properties is of utmost importance to understand the behavior and evolution of hot and dense QCD matter. Various thermodynamic properties of strongly interacting nuclear matter have been estimated from the first principle lattice QCD (lQCD) approach. However, the applicability of lQCD breaks down at high baryochemical potential due to the fermion sign problem [1, 2]. An alternative to the lQCD approach at low temperatures (up to 150 MeV) is the Hadron Resonance Gas (HRG) model. The HRG model has been observed to agree with the lQCD results for temperatures up to $T \simeq 140 - 150$ MeV at zero baryochemical potential [3–8]. The HRG model is thus a better alternative to study the baryon-rich environments at low-temperature regimes [9–12].

In an ideal HRG model [13–16], the hadrons are assumed to be point-like particles with no interaction between them. However, this assumption is very simplistic and fails to describe the lQCD data at temperatures above $T \simeq 150$ MeV, where the hadrons meltdown and the HRG model reach their limits. Although this shortcoming of the HRG model can be easily ignored while

studying the thermodynamic properties, however, while estimating various charge fluctuations at higher order, the shortcomings of the HRG model are not trivial. Recently, much focus has been diverting towards an interacting hadron resonance gas model as they extend the region of agreement with lQCD data due to the interactions between the hadrons. Excluded volume hadron resonance gas (EVHRG) model assumes an eigenvolume parameter for the hadrons, which essentially mimics a repulsive interaction in the hadron gas [17–27]. Unequal sizes of different hadrons species are handled by modified excluded volume hadron resonance gas (MEVHRG) model [28–30]. Similarly, the mean-field hadron resonance gas (MFHRG) model introduces a repulsive interaction potential in the hadronic medium [31–33]. There are also various other improvements to the HRG model in literature, such as the Lorentz modified excluded volume hadron resonance gas (LMEVHRG) model [34], where the hadrons are treated as Lorentz contracted particles, and the effective thermal mass hadron resonance gas (THRG) model [35], where the hadrons gain effective mass with temperature. However, the most successful improvement to the model which explains the lQCD results is the van der Waals hadron resonance gas (VDWHRG) model [36–40]. This model assumes a van der Waals-type interaction between the hadrons, having both attractive and repulsive parts. The VDWHRG model effectively explains the lQCD data up to $T \simeq 180$ MeV. From this, we can infer that van der Waals interaction does play a crucial role in the hadronic systems at high temperatures. Moreover, the VDWHRG model has been recently used to estimate various thermodynamic and transport properties [36, 39, 40], along with fluctuations of conserved charges [36], which show a good agreement with the lQCD estimations. In addition, there are several studies exploring the liquid-gas phase transition using the VDWHRG model, locating a possible critical point for the phase transition [36, 37, 39]

*Corresponding Author Email: Raghunath.Sahoo@cern.ch

A unique consequence of the peripheral heavy-ion collisions is that a strong transient magnetic field ($\sim m_\pi^2 \sim 10^{18}$ G) is expected to be formed due to the motion of the spectator protons. The strength of the magnetic field may reach up to the order of $0.1m_\pi^2$, m_π^2 , $15m_\pi^2$ for SPS, RHIC, and LHC energies, respectively [41]. This magnetic field decays with time and can, in principle, affect the thermodynamic and transport properties of the evolving partonic and hadronic matter [41–44]. The strong magnetic field, which can reach hadronic scales, has a significant effect on the transition properties and equation of state. Such intense magnetic fields are predicted to occur in compact neutron stars [45, 46] and during the early universe’s electroweak transition [47, 48]. The interaction between the strong dynamics and the external magnetic field leads to exciting new phenomena, such as the chiral magnetic effect [49, 50] and a reduction of the transition temperature as the magnetic field increases [51]. Furthermore, magnetic catalysis [52] and inverse magnetic catalysis [53, 54] can affect the phase diagram of QCD matter. Thus, it is crucial to study the effect of an external magnetic field on both the deconfined and confined phases of the matter formed in high-energy collisions. Thermodynamic properties of the system, such as pressure (P), energy density (ε), entropy density (s), speed of sound (c_s), and specific heat (c_v) will get modified due to the effect of an external magnetic field. All these observables help us characterize the systems produced in ultra-relativistic collisions. Moreover, the system will also develop some magnetization (\mathcal{M}), which will help us to understand whether the system is diamagnetic or paramagnetic. Apart from these, the magnetic susceptibility (χ_M^2) and magnetic permeability (μ_r) are also essential observables that can give us useful information about the system under consideration [16, 55–62]. With the help of magnetic permeability and electric susceptibility, one can, in principle, get an idea about the optical properties of the system. Thus, one must study the above-mentioned observables to better understand the nature and behavior of both the hadronic and partonic medium formed in peripheral heavy-ion collisions.

Several works in literature concern with the study of the matter formed in ultra-relativistic collisions in the presence of a constant external magnetic field. In ref. [61], a detailed analysis of the hot and dense QCD matter in the presence of an external magnetic field has been done with the lQCD approach. The results from the SU(3) Polyakov linear-sigma model (PLSM) has also been contrasted with the existing lQCD estimations [63]. In addition, in ref. [64, 65] the authors use the HRG and EVHRG models in the presence of constant external magnetic fields to estimate the fundamental thermodynamic quantities such as pressure, energy density, and magnetization. Moreover, in ref. [16], the authors discuss the effect of external magnetic field on the correlations and fluctuations of the hadron gas. An interesting study has been conducted by assuming an away from equilibrium

scenario by employing the non-extensive Tsallis statistics, and then the basic thermodynamic quantities have been estimated [66]. In the present study, we use the van der Waals hadron resonance gas model, an improved and new approach to study the hadronic medium of high-energy collisions. Furthermore, van der Waals interaction leads to a liquid-gas phase transition in the system along with a critical point. We can take advantage of this fact and study the QCD phase diagram. In literature, the QCD phase transition in the $T - \mu_B$ plane has been studied extensively from various models, including the VDWHRG model [36, 39]. A similar QCD phase transition in the $T - eB$ plane is also important to understand the QCD matter and its consequences. There are few studies where the authors have used various models to map the phase diagram. This study uses the hadron gas with van der Waals interaction and explores the possible critical point in the $T - eB - \mu_B$ plane. This paper is organized as follows. The section II gives a detailed calculation of the thermodynamic observables and susceptibilities within the ambit of a VDWHRG model under an external magnetic field. In section III, we give the detailed calculation of the vacuum contribution to the thermodynamic observables due to the external magnetic field. We discuss the results in section IV and briefly summarize our work in section V.

II. FORMULATION

The ideal HRG formalism considers hadrons to be point particles with no interactions between them. Under this formalism, the partition function of i th particle species in a Grand Canonical Ensemble (GCE) is given as [23]

$$\ln Z_i^{id} = \pm V g_i \int \frac{d^3 p}{(2\pi)^3} \ln \{1 \pm \exp[-(E_i - \mu_i)/T]\}, \quad (1)$$

where, T is the temperature of the system and V represents the volume. The notations g_i , $E_i = \sqrt{p^2 + m_i^2}$, m_i and μ_i are for the degeneracy, energy, mass, and chemical potential of the i th hadron, respectively. Here, id refers to the ideal. The plus and minus signs (\pm) correspond to baryons and mesons, respectively. μ_i is further expanded in terms of the baryonic, strangeness, and charge chemical potentials (μ_B , μ_S and μ_Q , respectively) and the corresponding conserved numbers (B_i , S_i and Q_i) as,

$$\mu_i = B_i \mu_B + S_i \mu_S + Q_i \mu_Q. \quad (2)$$

The total Grand Canonical partition function of non-interacting hadron resonance gas is the sum of partition functions of all hadrons and resonances [13, 23],

$$\ln Z^{id} = \sum_i \ln Z_i^{id}. \quad (3)$$

The free energy density of the ideal HRG model can be written in terms of partition function as,

$$f^{id} = -T \ln Z^{id}. \quad (4)$$

The ideal pressure is defined as the negative of free energy density,

$$P^{id} = -f^{id}. \quad (5)$$

The explicit form of thermodynamic pressure P_i , energy density ε_i , number density n_i , and entropy density s_i in the ideal HRG formalism can now be obtained as,

$$P_i^{id}(T, \mu_i) = \pm T g_i \int \frac{d^3 p}{(2\pi)^3} \ln \{1 \pm \exp[-(E_i - \mu_i)/T]\} \quad (6)$$

$$\varepsilon_i^{id}(T, \mu_i) = g_i \int \frac{d^3 p}{(2\pi)^3} \frac{E_i}{\exp[(E_i - \mu_i)/T] \pm 1} \quad (7)$$

$$n_i^{id}(T, \mu_i) = g_i \int \frac{d^3 p}{(2\pi)^3} \frac{1}{\exp[(E_i - \mu_i)/T] \pm 1} \quad (8)$$

$$s_i^{id}(T, \mu_i) = \pm g_i \int \frac{d^3 p}{(2\pi)^3} \left[\ln \{1 \pm \exp[-(E_i - \mu_i)/T]\} \pm \frac{(E_i - \mu_i)/T}{\exp[(E_i - \mu_i)/T] \pm 1} \right]. \quad (9)$$

In the presence of a magnetic field (for simplicity, suppose the magnetic field is pointing along z direction), the single particle energy for the charged and neutral particles is given as [64, 65, 67],

$$E_{c,i}^z(p_z, k, s_z) = \sqrt{p_z^2 + m_i^2 + 2|Q_i|B \left(k + \frac{1}{2} - s_z \right)}, Q_i \neq 0 \quad (10)$$

$$E_{n,i}(p) = \sqrt{p^2 + m_i^2}, \quad Q_i = 0, \quad (11)$$

where, Q_i is the charge of the i^{th} particle and s_z is the component of spin s in the direction of magnetic field B and k is the Landau level. The subscripts 'c' and 'n' are for charged and neutral particles.

In the presence of Landau level, one writes the three-dimensional integral as one-dimensional integral [68, 69],

$$\int \frac{d^3 p}{(2\pi)^3} = \frac{|Q|B}{2\pi^2} \sum_k \sum_{s_z} \int_0^\infty dp_z. \quad (12)$$

Now, in the presence of a finite magnetic field, the free energy of the system can be written as [70, 71]

$$f = \varepsilon - Ts - QB \cdot \mathcal{M}, \quad (13)$$

where, \mathcal{M} is the magnetization. Further, in the presence of finite baryochemical potential, the above equation becomes,

$$f = \varepsilon - Ts - QB \cdot \mathcal{M} - \mu n, \quad (14)$$

The n is the number density. The above equation satisfies the differential relations,

$$s = -\frac{\partial f}{\partial T}, \quad \mathcal{M} = -\frac{\partial f}{\partial (QB)}, \quad n = -\frac{\partial f}{\partial \mu}. \quad (15)$$

In general, the free energy density of the system contains contributions from both thermal and vacuum parts.

$$f = f_{vac} + f_{th}, \quad (16)$$

f_{vac} and f_{th} are the vacuum and thermal part of free energy density, respectively. f_{vac} is defined as the free energy density at zero temperature and finite magnetic field, and f_{th} is the free energy at finite temperature and finite magnetic field.

Now, the thermal part of the thermodynamic pressure, energy density, number density, and entropy density, i.e., Eqs. (6), (7), (8), and (9) for charged particles in the presence of magnetic field can be modified using the Eq. (12),

$$P_{c,i}^{id,z}(T, \mu_i, B) = \pm \frac{T g_i |Q_i| B}{2\pi^2} \sum_k \sum_{s_z} \int_0^\infty dp_z \ln \{1 \pm \exp[-(E_{c,i}^z - \mu_i)/T]\} \quad (17)$$

$$\varepsilon_{c,i}^{id,z}(T, \mu_i, B) = \frac{g_i |Q_i| B}{2\pi^2} \sum_k \sum_{s_z} \int dp_z E_{c,i}^z \left[\frac{1}{\exp[(E_{c,i}^z - \mu_i)/T] \pm 1} \right] \quad (18)$$

$$n_{c,i}^{id,z}(T, \mu_i, B) = \frac{g_i |Q_i| B}{2\pi^2} \sum_k \sum_{s_z} \int dp_z \left[\frac{1}{\exp[(E_{c,i}^z - \mu_i)/T] \pm 1} \right] \quad (19)$$

$$s_{c,i}^{id,z}(T, \mu_i, B) = \pm \frac{g_i |Q_i| B}{2\pi^2} \sum_k \sum_{s_z} \int dp_z \left[\ln \{1 \pm \exp[-(E_{c,i}^z - \mu_i)/T]\} \pm \frac{(E_{c,i}^z - \mu_i)/T}{\exp[(E_{c,i}^z - \mu_i)/T] \pm 1} \right]. \quad (20)$$

For neutral particles, these thermodynamic variables are calculated using the Eqs. (6), (7), (8), and (9). The total pressure, energy density, and entropy density of the system are due to the sum of contributions from the charged particles and neutral particles. Now, we can use

the above basic thermodynamic quantities to estimate other important observables.

The specific heat of the system is defined as the thermal variation of energy density at constant volume. It is defined as,

$$c_v = \left(\frac{\partial \varepsilon}{\partial T} \right)_V. \quad (21)$$

The squared speed of sound is defined as the change in pressure of a system as a function of a change in energy density at constant entropy density per number density, i.e., s/n . Mathematically, the adiabatic squared speed of sound is defined as,

$$c_s^2 = \left(\frac{\partial P}{\partial \varepsilon} \right)_{s/n} = \frac{s}{c_v}. \quad (22)$$

In the presence of both magnetic field and chemical potential, the squared speed of sound (c_s^2) is defined as,

$$c_s^2(T, \mu, QB) = \frac{\frac{\partial P}{\partial T} + \frac{\partial P}{\partial \mu} \frac{\partial \mu}{\partial T} + \frac{\partial P}{\partial(QB)} \frac{\partial(QB)}{\partial T}}{\frac{\partial \varepsilon}{\partial T} + \frac{\partial \varepsilon}{\partial \mu} \frac{\partial \mu}{\partial T} + \frac{\partial \varepsilon}{\partial(QB)} \frac{\partial(QB)}{\partial T}} \quad (23)$$

where,

$$\frac{\partial(QB)}{\partial T} = \frac{s \frac{\partial n}{\partial T} - n \frac{\partial s}{\partial T}}{n \frac{\partial s}{\partial(QB)} - s \frac{\partial n}{\partial(QB)}} \quad (24)$$

and,

$$\frac{\partial \mu}{\partial T} = \frac{s \frac{\partial n}{\partial T} - n \frac{\partial s}{\partial T}}{n \frac{\partial s}{\partial \mu} - s \frac{\partial n}{\partial \mu}}. \quad (25)$$

A detailed derivation of the squared speed of sound in the presence of a finite baryochemical potential and an external magnetic field is given in the appendix A.

The magnetization of the system can also be obtained from the following equation,

$$\mathcal{M} = \frac{\varepsilon_{tot} - \varepsilon}{QB}, \quad (26)$$

where, $\varepsilon_{tot} = \varepsilon_{c,i}^z + \varepsilon_{n,i}$ is the energy density of the system in the presence of the magnetic field. $\varepsilon_{c,i}^z$, and $\varepsilon_{n,i}$ are the energy density of charged and neutral particles in the presence of a magnetic field, respectively. ε is the free energy density in the absence of a magnetic field.

We now proceed toward the estimation of the optical properties of a hadronic system. The derivative of magnetization with respect to the magnetic field is called magnetic susceptibility and is given by,

$$\chi_M^2 = \frac{\partial \mathcal{M}}{\partial(QB)} = \frac{\partial^2 P}{\partial(QB)^2}. \quad (27)$$

From heavy-ion collision (HIC) perspectives, fluctuations of conserved charges have comparable importance

as magnetic susceptibility since they play a vital role in describing QCD phase transition. The n th-order susceptibility is defined as,

$$\chi_{B/Q/S}^n = \frac{\partial^n \left(\frac{P}{T^4} \right)}{\partial \left(\frac{\mu_{B/Q/S}}{T} \right)^n}. \quad (28)$$

The second-order susceptibility corresponding to the electric charge is called electrical susceptibility, and is given by,

$$\chi_Q^2 = \frac{1}{T^2} \frac{\partial^2 P}{\partial \mu_Q^2} \quad (29)$$

The explicit forms of χ_M^2 and χ_Q^2 are shown in appendix B and C, respectively. Now, one can, in principle be able to estimate the refractive index of a hadron gas by using the above information.

To include interactions in the hadronic system, we take advantage of the van der Waals equation of state. The ideal HRG model can be modified to include van der Waals interactions between particles by the introduction of the attractive and repulsive parameters a and b , respectively. This modifies the pressure and number density obtained in ideal HRG iteratively as follows [36, 37, 72]

$$P(T, \mu) = P^{id}(T, \mu^*) - an^2(T, \mu), \quad (30)$$

where, the $n(T, \mu)$ is the VDW particle number density given by

$$n(T, \mu) = \frac{\sum_i n_i^{id}(T, \mu^*)}{1 + b \sum_i n_i^{id}(T, \mu^*)}. \quad (31)$$

Here, i runs over all hadrons and μ^* is the modified chemical potential given by,

$$\mu^* = \mu - bP(T, \mu) - abn^2(T, \mu) + 2an(T, \mu). \quad (32)$$

It is to be noted that the repulsive parameter is usually attributed to be related to the hardcore radius of the particle, r , by the relation $b = 16\pi r^3/3$. At the same time, the VDW parameter, a , represents the attractive interaction at an intermediate range.

The entropy density $s(T, \mu)$ and energy density $\varepsilon(T, \mu)$ in VDWHRG can now be obtained as,

$$s(T, \mu) = \frac{s^{id}(T, \mu^*)}{1 + bn^{id}(T, \mu^*)} \quad (33)$$

$$\varepsilon(T, \mu) = \frac{\sum_i \varepsilon_i^{id}(T, \mu^*)}{1 + b \sum_i n_i^{id}(T, \mu^*)} - an^2(T, \mu) \quad (34)$$

The initial form of VDWHRG excluded interactions between baryon-antibaryon pairs and in between pairs involving at least one meson [36–38, 72]. The baryon-antibaryon interactions were ignored under the assumption that annihilation processes dominate [23, 38]. Meson interactions were ignored as their inclusion led to

a suppression of thermodynamic quantities and couldn't explain the IQCD data at vanishing μ_B towards high temperatures [38]. The attractive and repulsive parameters, in this case, were derived either from properties of the ground state of nuclear matter [37] or by fitting the IQCD results for different thermodynamic quantities [36, 39]. A formalism including the effect of meson-meson interactions through a hardcore repulsive radius (r_M) [39] was developed where a simultaneous fit to the IQCD values was done to obtain the values of a and b . The VDW parameters were considered to be fixed for all values of μ_B and T in each of these implementations. The total pressure in the VDWHRG model is then written as [36–39, 72],

$$P(T, \mu) = P_M(T, \mu) + P_B(T, \mu) + P_{\bar{B}}(T, \mu). \quad (35)$$

Here, the $P_M(T, \mu)$, $P_{B(\bar{B})}(T, \mu)$ are the contributions to pressure from mesons and (anti)baryons, respectively, and are given by,

$$P_M(T, \mu) = \sum_{i \in M} P_i^{id}(T, \mu^{*M}), \quad (36)$$

$$P_B(T, \mu) = \sum_{i \in B} P_i^{id}(T, \mu^{*B}) - an_B^2(T, \mu), \quad (37)$$

$$P_{\bar{B}}(T, \mu) = \sum_{i \in \bar{B}} P_i^{id}(T, \mu^{*\bar{B}}) - an_{\bar{B}}^2(T, \mu). \quad (38)$$

Here, M , B , and \bar{B} represent mesons, baryons, and anti-baryons, respectively. μ^{*M} is the modified chemical potential of mesons because of the excluded volume correction, and μ^{*B} and $\mu^{*\bar{B}}$ are the modified chemical potentials of baryons and anti-baryons due to VDW interactions [39]. Considering the simple case of vanishing electric charge and strangeness chemical potentials, $\mu_Q = \mu_S = 0$, the modified chemical potential for mesons and (anti)baryons can be obtained from Eq. (2) and Eq. (33) as;

$$\mu^{*M} = -bP_M(T, \mu), \quad (39)$$

$$\mu^{*B(\bar{B})} = \mu_{B(\bar{B})} - bP_{B(\bar{B})}(T, \mu) - abn_{B(\bar{B})}^2 + 2an_{B(\bar{B})}, \quad (40)$$

where n_M , n_B and $n_{\bar{B}}$ are the modified number densities of mesons, baryons, and anti-baryons, respectively, which are given by,

$$n_M(T, \mu) = \frac{\sum_{i \in M} n_i^{id}(T, \mu^{*M})}{1 + b \sum_{i \in M} n_i^{id}(T, \mu^{*M})}, \quad (41)$$

$$n_{B(\bar{B})}(T, \mu) = \frac{\sum_{i \in B(\bar{B})} n_i^{id}(T, \mu^{*B(\bar{B})})}{1 + b \sum_{i \in B(\bar{B})} n_i^{id}(T, \mu^{*B(\bar{B})})}. \quad (42)$$

For this work, the parameters in the model are taken as $a = 0.926 \text{ GeV fm}^3$ and $b = (16/3)\pi r^3$, where the hardcore radius r is replaced by $r_M = 0.2 \text{ fm}$ and $r_{B,(\bar{B})} = 0.62 \text{ fm}$, respectively for mesons and (anti)baryons [39]. Now, we take the magnetic field-modified total ideal pressure, energy density, and entropy density and use them in the respective VDW equations to estimate the required thermodynamic observables.

III. RENORMALIZATION OF VACUUM PRESSURE

As we discussed in the previous section, the total pressure (negative of the total free energy density) of the system is due to both the thermal and vacuum components, i.e.

$$P_{total} = P_{th}(T, eB) + \Delta P_{vac}(T = 0, eB) \quad (43)$$

where $P_{th}(T, eB)$ is the thermal part of the pressure, which is the sum of the pressure due to both charged and neutral particles. In the presence of a magnetic field, the thermal part of the pressure for charged and neutral particles are calculated using Eqs. (17), and (6), respectively. In this section, we will calculate the vacuum contribution of pressure in the presence of an external magnetic field using a dimensional regularization method. The vacuum pressure term is ultraviolet divergent, and it requires appropriate regularization to extract meaningful physical information[64, 65, 73]. As a result, magnetic field-dependent and independent components must be distinguished using an appropriate regularization technique.

In the presence of an external magnetic field, the vacuum pressure for a charged spin- $\frac{1}{2}$ particle is given by [64, 65, 73],

$$P_{vac}(S = 1/2, B) = \frac{1}{2} \sum_{k=0}^{\infty} g_k \frac{|Q|B}{2\pi} \int_{-\infty}^{\infty} \frac{dp_z}{2\pi} E_{p,k}(B), \quad (44)$$

where $g_k = 2 - \delta_{k0}$ is the degeneracy of k^{th} Landau level. We have added and subtracted the lowest Landau level contribution (i.e., $k = 0$) from the above equation, and we get

$$P_{vac}(S = 1/2, B) = \frac{1}{2} \sum_{k=0}^{\infty} 2 \frac{|Q|B}{2\pi} \int_{-\infty}^{\infty} \frac{dp_z}{2\pi} \left[E_{p,k}(B) - \frac{E_{p,0}(B)}{2} \right]. \quad (45)$$

A dimensional regularization method [74] is used to regularize the ultraviolet divergence of vacuum pressure. In $d - \varepsilon$ dimension Eq. (45) can be written as

$$P_{\text{vac}}(S = 1/2, B) = \sum_{k=0}^{\infty} \frac{|Q|B}{2\pi} \mu^\varepsilon \int_{-\infty}^{\infty} \frac{d^{1-\varepsilon} p_z}{(2\pi)^{1-\varepsilon}} \left[\sqrt{p_z^2 + m^2} - 2|Q|Bk - \sqrt{p_z^2 + m^2} \right], \quad (46)$$

In the preceding equation, μ sets the dimension to one. The integration can be carried out using the usual d -dimensional formulae [74, 75].

$$\int_{-\infty}^{\infty} \frac{d^d p}{(2\pi)^d} \left[p^2 + m^2 \right]^{-A} = \frac{\Gamma[A - \frac{d}{2}]}{(4\pi)^{d/2} \Gamma[A] (m^2)^{(A - \frac{d}{2})}}. \quad (47)$$

Integration of the first term in Eq. (46) gives

$$I_1 = \sum_{k=0}^{\infty} \frac{|Q|B}{2\pi} \mu^\varepsilon \int_{-\infty}^{\infty} \frac{d^{1-\varepsilon} p_z}{(2\pi)^{1-\varepsilon}} \left[p_z^2 + m^2 - 2|Q|Bk \right]^{\frac{1}{2}} \\ = -\frac{(|Q|B)^2}{4\pi^2} \left(\frac{2|Q|B}{4\pi\mu} \right)^{-\frac{\varepsilon}{2}} \Gamma \left[-1 + \frac{\varepsilon}{2} \right] \zeta \left[-1 + \frac{\varepsilon}{2}, x \right] \quad (48)$$

where we denote $x \equiv \frac{m^2}{2|Q|B}$. The Landau infinite sum has been illustrated in terms of the Riemann-Hurwitz ζ -function

$$\zeta[z, x] = \sum_{k=0}^{\infty} \frac{1}{[x+k]^z}, \quad (49)$$

with the expansion [76, 77],

$$\zeta \left[-1 + \frac{\varepsilon}{2}, x \right] \approx -\frac{1}{12} - \frac{x^2}{2} + \frac{x}{2} + \frac{\varepsilon}{2} \zeta'(-1, x) + \mathcal{O}(\varepsilon^2) \quad (50)$$

and the asymptotic behavior of the derivative [76, 77],

$$\zeta'(-1, x) = \frac{1}{12} - \frac{x^2}{4} + \left(\frac{1}{12} - \frac{x}{2} + \frac{x^2}{2} \right) \ln(x) + \mathcal{O}(x^{-2}). \quad (51)$$

The expansion of Γ -function around some negative integers is given by,

$$\Gamma \left[-1 + \frac{\varepsilon}{2} \right] = -\frac{2}{\varepsilon} + \gamma - 1 + \mathcal{O}(\varepsilon), \quad (52)$$

and,

$$\Gamma \left[-2 + \frac{\varepsilon}{2} \right] = \frac{1}{\varepsilon} - \frac{\gamma}{2} + \frac{3}{4} + \mathcal{O}(\varepsilon). \quad (53)$$

Here, γ is the Euler constant. The limiting expression for natural is,

$$\lim_{\varepsilon \rightarrow 0} a^{-\varepsilon/2} \approx 1 - \frac{\varepsilon}{2} \ln(a). \quad (54)$$

Eq. (48) can be written as expressed as using the expansion of the Γ -function and ζ -function

$$I_1 = -\frac{(|Q|B)^2}{4\pi^2} \left[-\frac{2}{\varepsilon} + \gamma - 1 + \ln \left(\frac{2|Q|B}{4\pi\mu^2} \right) \right] \\ \left[-\frac{1}{12} - \frac{x^2}{2} + \frac{x}{2} + \frac{\varepsilon}{2} \zeta'(-1, x) + \mathcal{O}(\varepsilon^2) \right] \quad (55)$$

The second term in Eq. (46) can be simplified in the same way, and we obtain,

$$I_2 = \sum_{k=0}^{\infty} \frac{|Q|B}{2\pi} \mu^\varepsilon \int_{-\infty}^{\infty} \frac{d^{1-\varepsilon} p_z}{(2\pi)^{1-\varepsilon}} \left[p_z^2 + m^2 \right]^{\frac{1}{2}} \\ = \frac{(|Q|B)^2}{4\pi^2} \left[-\frac{x}{\varepsilon} - \frac{(1-\gamma)}{2} x + \frac{x}{2} \ln \left(\frac{2|Q|B}{4\pi\mu^2} \right) + \frac{x}{2} \ln(x) \right]. \quad (56)$$

Hence, the vacuum pressure in the presence of an external magnetic field becomes

$$P_{\text{vac}}(S = 1/2, B) = \frac{(|Q|B)^2}{4\pi^2} \left[\zeta'(-1, x) - \frac{2}{12\varepsilon} - \frac{(1-\gamma)}{12} \right. \\ \left. - \frac{x^2}{\varepsilon} - \frac{(1-\gamma)}{2} x^2 + \frac{x}{2} \ln(x) \right. \\ \left. + \frac{x^2}{2} \ln \left(\frac{2|Q|B}{4\pi\mu^2} \right) + \frac{1}{12} \ln \left(\frac{2|Q|B}{4\pi\mu^2} \right) \right]. \quad (57)$$

Divergence is still evident in the preceding expression. As a result, we add and deduct the $B = 0$ contribution from it. To carry out the renormalization of the $B > 0$ pressure, the $B = 0$ contribution must be determined. The vacuum pressure in $d = 3 - \varepsilon$ dimensions at $B = 0$ is given by

$$P_{\text{vac}}(S = 1/2, B = 0) = \mu^\varepsilon \int \frac{d^{3-\varepsilon} p}{(2\pi)^{3-\varepsilon}} (p^2 + m^2)^{\frac{1}{2}} \\ = \frac{(|Q|B)^2}{4\pi^2} \left(\frac{2|Q|B}{4\pi\mu^2} \right)^{-\frac{\varepsilon}{2}} \Gamma \left(-2 + \frac{\varepsilon}{2} \right) x^{2-\frac{\varepsilon}{2}}. \quad (58)$$

Above Eq. (58) can be further simplified by using Γ -function expansion from Eq. (52),

$$P_{\text{vac}}(S = 1/2, B = 0) = -\frac{(|Q|B)^2}{4\pi^2} x^2 \left[\frac{1}{\varepsilon} + \frac{3}{4} - \frac{\gamma}{2} \right. \\ \left. - \frac{1}{2} \ln \left(\frac{2|Q|B}{4\pi\mu^2} \right) - \frac{1}{2} \ln(x) \right] \quad (59)$$

Now, we add and subtract Eq. (59) from (57), we get the regularized pressure with the vacuum part, and the magnetic field-dependent part separated as,

$$P_{\text{vac}}(S = 1/2, B) = P_{\text{vac}}(1/2, B = 0) + \Delta P_{\text{vac}}(1/2, B), \quad (60)$$

where,

$$\begin{aligned} \Delta P_{\text{vac}}(S = 1/2, B) &= \frac{(|Q|B)^2}{4\pi^2} \left[-\frac{2}{12\varepsilon} + \frac{\gamma}{12} \right. \\ &+ \frac{1}{12} \ln\left(\frac{m^2}{4\pi\mu^2}\right) + \frac{x}{2} \ln(x) - \frac{x^2}{2} \ln(x) \\ &\left. + \frac{x^2}{4} - \frac{\ln(x)+1}{12} + \zeta'(-1, x) \right]. \quad (61) \end{aligned}$$

The field contribution given by the Eq. (61) is, however, divergent due to the existence of the magnetic field dependent term $\frac{B^2}{\varepsilon}$ [80–82]. We eliminate this divergence by redefining field-dependent pressure contribution to include magnetic field contribution.

$$\Delta P_{\text{vac}}^r = \Delta P_{\text{vac}}(B) - \frac{B^2}{2}. \quad (62)$$

The divergences are absorbed into the renormalization of the electric charge and the magnetic field strength [64],

$$B^2 = Z_e B_r^2; \quad e^2 = Z_e^{-1} e_r^2; \quad e_r B_r = |Q|B, \quad (63)$$

Where the electric charge renormalization constant is

$$Z_e\left(S = \frac{1}{2}\right) = 1 + \frac{1}{2} e_r^2 \left[-\frac{2}{12\varepsilon} + \frac{\gamma}{12} + \frac{1}{12} \ln\left(\frac{m_*}{4\pi\mu^2}\right) \right]. \quad (64)$$

We fix $m_* = m$, i.e. the particle's physical mass. Thus, the contribution of the renormalized field-dependent pressure in the absence of a pure magnetic field ($\frac{B^2}{2}$) is,

$$\begin{aligned} \Delta P_{\text{vac}}^r(S = 1/2, B) &= \frac{(|Q|B)^2}{4\pi^2} \left[\zeta'(-1, x) + \frac{x}{2} \ln(x) \right. \\ &\left. - \frac{x^2}{2} \ln(x) + \frac{x^2}{4} - \frac{\ln(x)+1}{12} \right] \quad (65) \end{aligned}$$

Using a similar technique, the renormalized magnetic field-dependent pressure for spin-zero and spin-one particles can be calculated. These terms are crucial in determining the magnetization of hadronic matter. The vacuum pressure is affected by the charge, mass, and spin of the particles. As a result, the total vacuum pressure of a hadron gas is calculated by adding the vacuum pressures of all particles taken into account.

For spin-zero particles, the regularized vacuum pressure is,

$$\begin{aligned} \Delta P_{\text{vac}}^r(s = 0, B) &= -\frac{(|Q|B)^2}{8\pi^2} \left[\zeta'(-1, x + 1/2) - \frac{x^2}{2} \ln(x) \right. \\ &\left. + \frac{x^2}{4} + \frac{\ln(x)+1}{24} \right]. \quad (66) \end{aligned}$$

Similarly, for spin-one particles,

$$\begin{aligned} \Delta P_{\text{vac}}^r(s = 1, B) &= -\frac{3}{8\pi^2} (|Q|B)^2 \left[\zeta'(-1, x - 1/2) \right. \\ &+ \frac{(x+1/2)}{3} \ln(x+1/2) \\ &+ \frac{2}{3} (x-1/2) \ln(x-1/2) - \frac{x^2}{2} \ln(x) \\ &\left. + \frac{x^2}{4} - \frac{7}{24} (\ln(x)+1) \right]. \quad (67) \end{aligned}$$

So, the total magnetic field-dependent vacuum pressure becomes,

$$\begin{aligned} \Delta P_{\text{vac}} &= \Delta P_{\text{vac}}^r(s = 0, B) + \Delta P_{\text{vac}}^r(S = 1/2, B) \\ &+ \Delta P_{\text{vac}}^r(s = 1, B). \quad (68) \end{aligned}$$

After computing the total vacuum pressure, the system's vacuum magnetization can be computed as follows:

$$\Delta \mathcal{M}_{\text{vac}} = \frac{\partial(\Delta P_{\text{vac}})}{\partial(|Q|B)}. \quad (69)$$

The explicit calculation of $\Delta \mathcal{M}_{\text{vac}}$ for spin-0, spin-1/2 and spin-1 particle are shown in appendix D. By using the formalism mentioned above in the above two sections, we estimate various thermodynamic observables for a hadron gas with van der Waals interaction.

IV. RESULTS AND DISCUSSION

In the present section, we discuss the results obtained from this study. It is important to note that we obtain all the results at $\mu_Q = 0$ and $\mu_S = 0$. So the chemical potential of the system is only due to μ_B . We explore the effect of the magnetic field on thermodynamic observables at both zero and finite baryon chemical potential values. This study includes all hadrons and resonances of spin-0, spin-1/2, and spin-1 up to a mass cut-off of 2.25 GeV according to particle data group [78]. One can obtain the van der Waals parameters by fitting the thermodynamic quantities, such as energy density, pressure, etc., in the VDWHRG model to the available lattice QCD data at zero magnetic fields [39]. In principle, the van der Waals parameters should change in the presence of the magnetic field as well as the baryochemical potential. However, changing a and b parameters as a function of eB as well as μ_B is non-trivial. We have neglected such dependencies in the current study. We calculate the thermodynamic quantities such as pressure, energy density, entropy density, specific heat, and squared speed of sound using their corresponding formulas as given in section II at zero and finite magnetic fields in the ideal HRG and VDWHRG models.

In the present work, we examine two different values of magnetic fields, i.e., $eB = 0.2 \text{ GeV}^2$ and $eB = 0.3 \text{ GeV}^2$

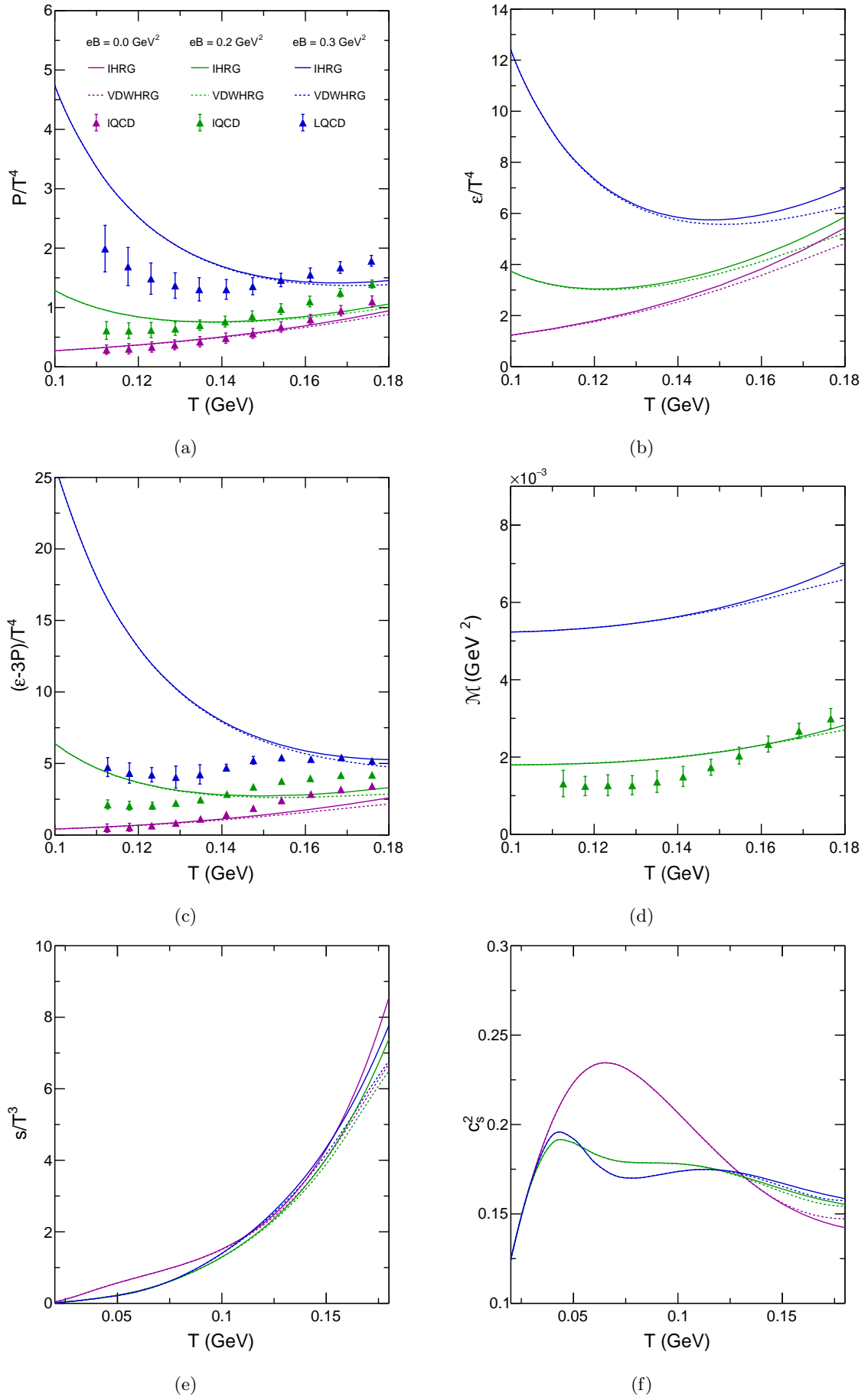


FIG. 1: (Color online) The equation of state in the ideal HRG (VDWHRG) model is shown in a solid line (dotted line). The variation (from left to right and downwards) of normalized pressure, energy density, trace anomaly, magnetization, entropy density, and squared speed of sound as functions of temperature at zero baryochemical potential ($\mu_B = 0$ GeV), for $eB = 0$ GeV² (magenta), $eB = 0.2$ GeV² (green), $eB = 0.3$ GeV² (blue). The lattice data

for our study. In the presence of a finite magnetic field, the system's total pressure contains a contribution from both the vacuum and the thermal part, while there is no such vacuum pressure contribution for a vanishing magnetic field. So, at $B \neq 0$ and $T=0$, the system has some non-vanishing pressure called vacuum pressure [64, 65]. The vacuum pressure for spin-0, spin-1/2, and spin-1 particles is calculated using Eqs. (65), (66), and (67). It is found that the vacuum pressure is positive for spin-0, spin-1/2, and spin-1 particles. The total vacuum pressure is obtained by summing over all spin states. In Fig.1(a), we show the scaled pressure as a function of temperature in ideal HRG and VDWHRG for both zero and finite magnetic fields and compare it with the IQCD data. We observe that the pressure calculated in HRG and VDWHRG slightly deviates from the IQCD calculation, but the temperature dependence seems to be preserved. This deviation at high temperatures may be due to the fact that we are not considering higher spin states in our calculations. One can observe that the normalized pressure increases with the temperature almost monotonically for a zero magnetic field, while for a finite magnetic field, it diverges at a lower temperature due to a finite vacuum contribution to the total pressure, both for the HRG and VDWHRG models. The pressure in the VDWHRG model is found to be suppressed slightly compared to the HRG model. However, we found that the total pressure of the system (without scaling with T^4) increases with temperature with an increase in a magnetic field. The lightest spin-0 particles (mainly dominated by pions(π^\pm, π^0)) have more contribution towards pressure compared to heavier spin-1 (ρ^\pm, ρ^0) and spin-1/2 (proton(p), neutron(n)) particles. In addition, it is noteworthy to mention that at lower temperatures, the thermal part of the pressure in the presence of a magnetic field is smaller than the pressure at a zero magnetic field. The vacuum pressure increases with an increase in the magnetic field, which is responsible for the monotonic increase in pressure with the magnetic field.

The total energy density in the presence of a magnetic field takes the form $\varepsilon^{total} = \varepsilon + QBM$ [42], where ε^{total} and ε represent the total energy density in the presence and absence of a magnetic field, respectively. Fig. 1(b) illustrates the variation of ε/T^4 as a function of T along with the magnetic field in the ideal HRG and VDWHRG models. The ε/T^4 is found to increase with magnetic field for a fixed value of temperature. The ε/T^4 also exhibits divergence behaviour at lower T similar to that of P/T^4 . It is found that there is a significant contribution of interactions after $T = 130$ GeV, as shown in Fig. 1(b). The energy density is found to be suppressed at higher temperatures in the VDWHRG model due to dominating repulsive interactions.

The variation of the interaction measure (or normalized trace anomaly) as a function of temperature in the presence of a magnetic field is shown in Fig. 1(c). It can be directly derived from the energy-momentum tensor T_μ^ν , and it is sensitive to the massive hadronic states [26].

For a perfect fluid, it is the sum of all diagonal elements of T_μ^ν . This parameter helps to determine the degrees of freedom of the system. We observe that the normalized trace anomaly diverges at a very low temperature, similar to the pressure and energy density. The magnetic field dependence of normalized trace anomaly is similar to normalized pressure and energy density and is comparable with the IQCD data [61].

Fig. 1(d) depicts the variation of magnetization as a function of temperature at zero μ_B . The sign of magnetization defines the magnetic property of the system under consideration. A positive value of magnetization indicates the paramagnetic behavior of hadronic matter, which indicates the attraction of hadronic matter in an external magnetic field. This paramagnetic behavior of hadronic matter is observed in both ideal HRG and VDWHRG models. From Fig. 1(d), it is observed that magnetization has a monotonic behavior with increasing temperature. This magnetization contains contributions from both thermal and vacuum parts. The vacuum part of magnetization is calculated using Eq. (69). The magnetization obtained for $eB = 0.2$ GeV² in HRG and VDWHRG model reasonably agrees with that of the IQCD simulation. At very low temperatures, the thermal part of magnetization is significantly less because of the less abundance of charged hadrons. In addition to that, it is also important to note that the magnetization of charged pseudo-scalars mesons (spin-0) is found to be negative. The magnetization of the hadronic matter becomes positive when the vector mesons (spin-1) and spin-1/2 baryons populate the hadronic matter at higher temperatures. It is also noteworthy to point out that we found even though the thermal part of magnetization is negative at lower temperatures, the total value of magnetization is always positive due to the vacuum contribution.

Fig. 1(e) shows the change in entropy density as a function of temperature at zero and a finite magnetic field. Entropy being the first derivative of pressure w.r.t. temperature, there is no vacuum contribution term in entropy density. The value of entropy density is very small (almost vanishes) at lower temperatures, and it starts to increase with temperature. One can also notice that entropy density shows minimal deviation with magnetic field even at high temperatures. The entropy density is found to be suppressed because of the magnetic field. The effect of interactions also suppresses the value of entropy density. This observation may be interesting for heavy ion collision (HIC) experiments since entropy acts as a proxy for particle multiplicity. Although there is no significant dependence of the magnetic field on entropy density, the effect of the magnetic field on the squared speed of sound can be clearly visualized from Fig. 1(f). The variation of the squared speed of sound as a function of temperature and the magnetic field is depicted at $\mu_B = 0$, and we notice that the c_s^2 exhibits a dip towards lower temperatures with a magnetic field. The minimum position of c_s^2 indicates the deconfinement transition tem-

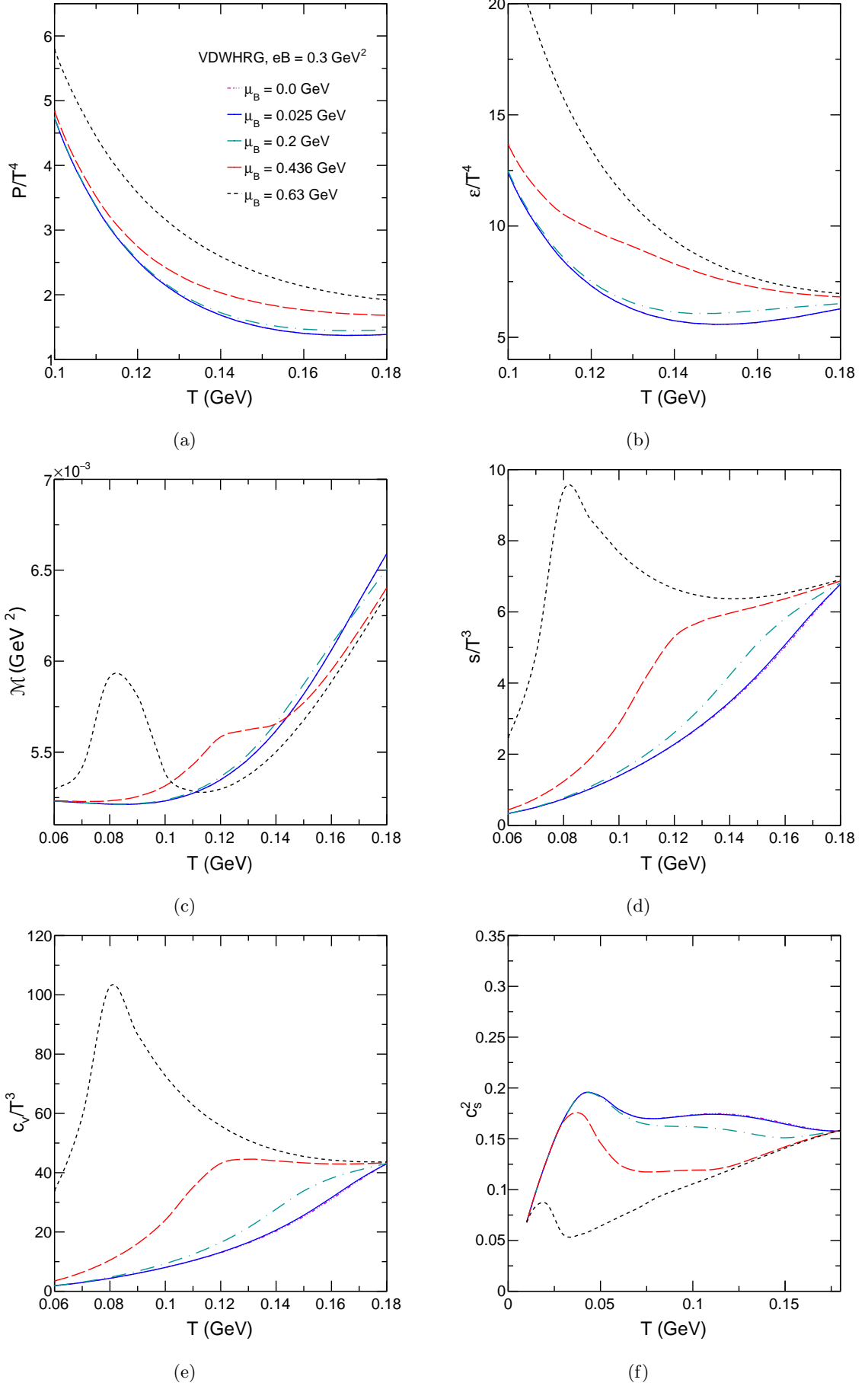


FIG. 2: (Color online) The variation (from left to right and downwards) of normalized pressure, energy density, magnetization, entropy density, specific heat, and squared speed of sound as functions of temperature at different baryochemical potentials for $eB = 0.3 \text{ GeV}^2$.

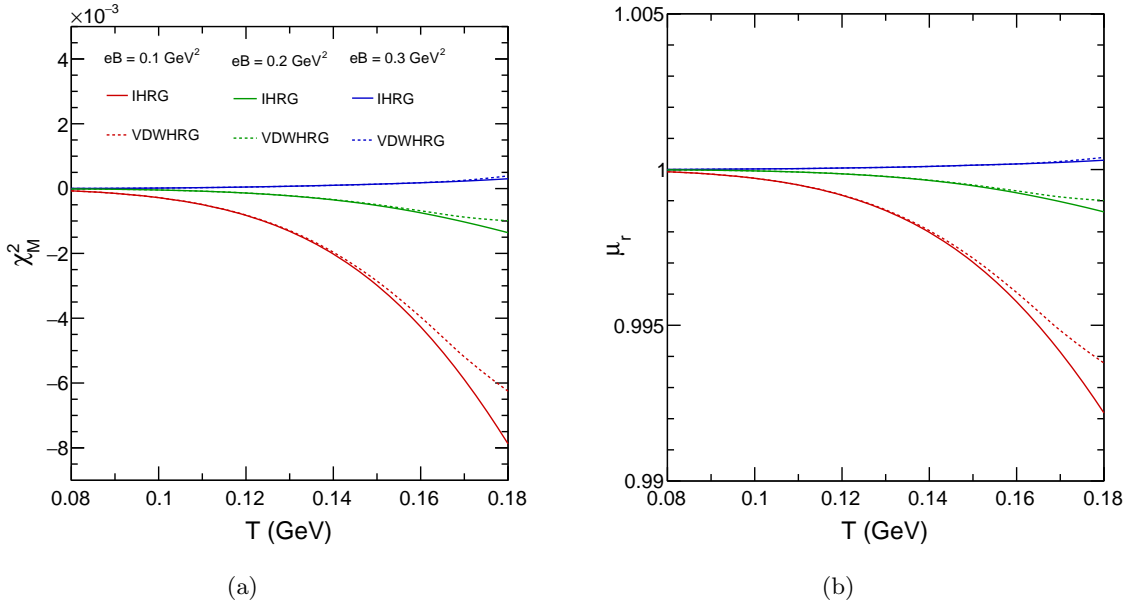


FIG. 3: (Color online) Magnetic susceptibility (left panel) and magnetic permeability (right panel) as functions of temperature for $eB = 0.1, 0.2, 0.3 \text{ GeV}^2$.

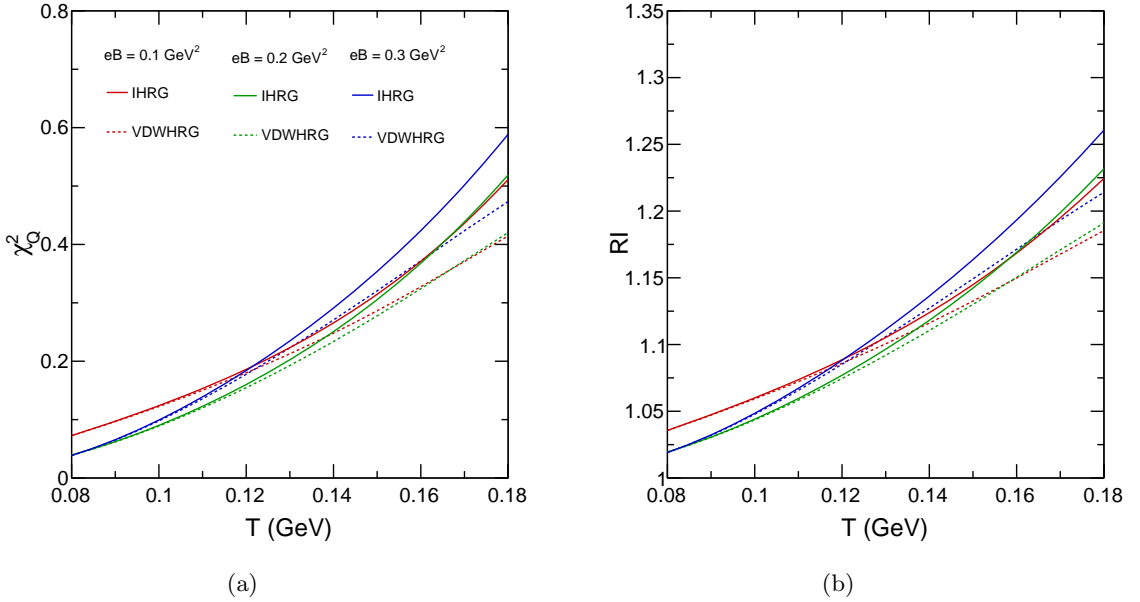


FIG. 4: (Color online) Electrical susceptibility (left panel) and refractive index (right panel) as functions of temperature for $eB = 0.1, 0.2, 0.3 \text{ GeV}^2$.

perature T_c .

Furthermore, we explore the variation of thermodynamic quantities in the presence of a finite chemical potential and a finite magnetic field. Fig. 2 depicts the variation of P/T^4 , ε/T^4 , \mathcal{M} , s , c_v and c_s^2 , respectively as functions of temperature for both finite values of chemical potential and magnetic field in the VDWHRG model. We set different values of μ_B , starting from 0.025 to 0.63 GeV, which correspond to the LHC, RHIC, FAIR, and

NICA experiments [83–86] at external magnetic field $eB = 0.3 \text{ GeV}^2$. It should be noted that the strength of eB also decreases with a decrease in collision energy. Here, we have not considered the variation of eB with collision energy, as it is not straightforward. One can observe that for lower values of chemical potential (up to 0.2 GeV), the behavior of thermodynamic quantities in the VDWHRG model is almost like that of the zero chemical potential, with a slight variation in magnitude. But,

there is a change in the behavior of some thermodynamic quantities observed for the higher value of chemical potential with magnetic field $eB = 0.3 \text{ GeV}^2$. From Fig. 2(a), it is observed that P/T^4 decreases monotonically with temperature for different values of chemical potential at $eB = 0.3 \text{ GeV}^2$. A similar kind of observation is made in the energy density, with a slight variation in its trend. The magnetization, entropy density, and specific heat are found to increase with increasing temperature for lower values of chemical potential, as shown in Fig. 2(b),(c),(d),(e), respectively. But for higher values of chemical potential, the trend seems very interesting. The monotonic decreasing (increasing) behavior starts deviating for chemical potential around 0.436 GeV and above, as depicted in energy density, magnetization, entropy density, and specific heat plots. Magnetization and entropy density, being the first-order derivatives of pressure with respect to magnetic field and temperature, respectively, show the behavior approaching a first-order phase transition at the higher chemical potential. The dependence of chemical potential on the squared speed of sound is quite interesting, as shown in Fig. 2(f). The squared speed of sound decreases with an increase in chemical potential, showing a minimum. This minimum position shifts towards lower temperatures with higher values of chemical potential.

In addition to thermodynamic results, it is crucial to understand the susceptibility of the medium under consideration, which is a sensitive probe for QCD phase transition. The magnetic susceptibility provides knowledge about the strength of the hadronic matter's induced magnetization. Its sign distinguishes diamagnet ($\chi_M^2 < 0$), which expels the external field, from paramagnet ($\chi_M^2 > 0$), which favors energetic exposure to the background field. In literature, the magnetic susceptibility of the HRG model is calculated through different approaches [56, 61]. Magnetic field dependence of magnetic susceptibility is also reported in the PNJL model [62]. Fig. 3(a) shows the magnetic field dependence of magnetic susceptibility with temperature. Since many of the thermodynamic quantities, including the fluctuation of conserved charges, are unaffected by the vacuum part [16], we neglect the vacuum contribution of susceptibilities in this study. One can observe that the magnetic susceptibility is negative for a lower value of magnetic field (e.g., $eB = 0.1 \text{ GeV}^2$ and $eB = 0.2 \text{ GeV}^2$), and its value tends towards positive for a higher magnetic field ($eB = 0.3 \text{ GeV}^2$) both for the ideal HRG and VDWHRG models. So a clear observation of the diamagnetic to paramagnetic transition happens in the VDWHRG model. It is quite an exciting consequence of the study of magnetic field dependence on magnetic susceptibility.

Taking magnetic susceptibility into account, one can calculate the magnetic permeability of the medium. The relative magnetic permeability is defined as $\mu_r = \frac{\mu}{\mu_0} = \frac{1}{1 - e^2 \chi_M^2}$ [60, 61]. This combination is equivalent to the ratio of the magnetic induction with the external field [60, 61]. Fig. 3(b) shows the magnetic field dependence of

relative magnetic permeability with temperature in the ideal HRG and VDWHRG models. It is observed that the relative magnetic permeability is close to unity at lower temperatures, and it starts deviating from unity (although the deviation is very small in magnitude) while going toward higher temperatures. The μ_r decreases with an increase in temperature at the lower magnetic field. Further, it starts to increase with the rise in the magnetic field.

We estimate the electrical susceptibility in HRG and VDWHRG models using Eq. (29). Fig. 4(a) shows the temperature dependence of electrical susceptibility for different values of the magnetic field. One observes that electrical susceptibility increases with an increase in temperature. With a higher magnetic field, the electrical susceptibility is found to be suppressed at lower temperatures, and it starts to increase beyond a certain value of temperature. This limiting temperature was found to decrease with an increase in the magnetic field. This is because the dominant contribution to susceptibility comes from spin-0 particles (π^\pm, k^\pm , etc.), and in the presence of a magnetic field, these particles are suppressed and don't contribute to susceptibility. As a result, the electric susceptibility decreases at low temperatures with an increase in the magnetic field. However, as temperature increases, the higher spin non-zero resonance particles ($\rho^\pm, k^{*\pm}, \Delta$, etc.) start contributing to susceptibility, and hence susceptibility is found to increase with the magnetic field at a higher temperature. Having the information of electrical susceptibility, one can easily calculate the electrical permittivity (or dielectric constant) of the medium under consideration using the relation $\epsilon_r = 1 + \chi_Q^2$ [79].

The knowledge of the relative permeability and electrical permittivity of the hadronic medium motivates us to calculate one of the most important optical properties, called the refractive index. In the literature, there are explicit calculations of the refractive index of the QGP medium [87, 88]. Although the refractive index of the medium is dispersion relation dependent, here we consider a simplistic picture to estimate the refractive index in a hadronic medium, which can be estimated using the most general relation, $RI = \sqrt{\epsilon_r \mu_r}$ [79]. Fig. 4(b) shows the refractive index variation as a function of temperature; the refractive index of the medium increases as the temperature increases. It is due to the fact that the number density of the system increases with temperature in the HRG model, and a denser medium causes a higher refractive index. The RI of the medium decreases with the magnetic field at lower temperatures and starts to increase at higher temperatures.

The ideal HRG model accounts only for the hadronic degrees of freedom without any phase transition to QGP. However, the inclusion of attractive and repulsive interaction through the VDWHRG model allows us to study the liquid-gas phase transition in the hadronic phase. In the literature, there are investigations of this liquid-gas phase transition in the VDWHRG model in the T - μ_B plane [36, 37, 39]. With different interaction parameters

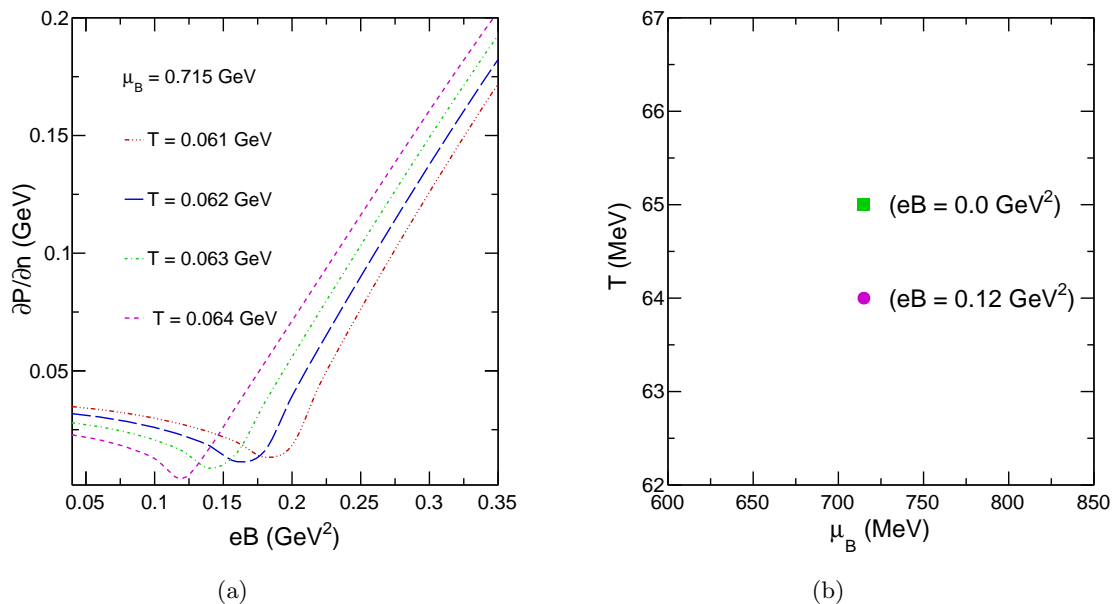


FIG. 5: (Color Online) The variation of $(\partial P/\partial n)_T$ as a function of magnetic field eB (left panel). The right panel shows the critical point of the liquid gas phase transition in the QCD phase diagram in the presence of a magnetic field.

a and b , the critical point of the phase transition is found to be different. Here, we explore the effect of the magnetic field on this critical point and study the liquid-gas phase transition in the $T - \mu_B - eB$ plane using the VD-WHRG model. In this analysis, we use the same van der Waals parameters as used in Ref. [39], where the authors observed the critical point around $T \approx 65$ MeV, and $\mu_B \approx 715$ MeV. Taking the same baryochemical potential, we explore the effect of the magnetic field to see its effect on the critical temperature. Fig. 5(a) shows the variation of the $(\partial P/\partial n)_T$ with eB for the same chemical potential, $\mu_B = 715$ MeV. Each curve is for different temperatures taken for the calculation. One can observe that the $(\partial P/\partial n)_T$ becomes zero at $T = 64$ MeV and $\mu_B = 715$ MeV for $eB = 0.12$ GeV². This marks the critical temperature below which the number density varies discontinuously, showing the 1st-order liquid-gas phase transition. To demonstrate the role of the magnetic field on the critical point, we plot the critical points in the $T - \mu_B$ plane in Fig. 5(b). The green square marker shows the critical point in the absence of the magnetic field [39], whereas the magenta circle marker shows the critical point in the presence of a magnetic field. One can observe that in the presence of the magnetic field, the critical point shifts towards lower temperatures, i.e., at $T = 0.064$ GeV, $\mu_B = 0.715$ GeV and $eB = 0.12$ GeV². This indicates that the magnetic field delays the liquid-gas phase transition. It is also important to note that the critical point now depends on three parameters, namely, temperature, T , baryochemical potential, μ_B , and the magnitude of the magnetic field, eB . Hence one can in principle be able to study the three-dimensional variation

of the critical point in the $T - \mu_B - eB$ plane.

V. SUMMARY

In this work, we explore the effect of a magnetic field on the thermodynamic properties of an interacting hadron resonance gas model at zero and finite chemical potential. The static finite magnetic field significantly affects pressure, energy density, trace anomaly, magnetization, and second-order conserved charge fluctuations such as electric and magnetic susceptibility. However, this effect is less significant on entropy density, specific heat, etc. We found that all thermodynamic quantities are suppressed because of interactions. The effect of higher baryon chemical potential on the thermodynamic variable is interesting. The magnetization, entropy density, specific heat, and speed of sound may indicate discontinuity behavior approaching a higher baryochemical potential, which suggests a phase transition in the VD-WHRG model. A clear observation of diamagnetic to paramagnetic transitions happens in our study. The electrical susceptibility is found to be suppressed because of the magnetic field at lower temperatures, and it slowly increases at higher temperatures. The optical property of the medium, like the refractive index, is also calculated and found to be increasing with temperature. A possible liquid-gas phase transition is also explored in the presence of a finite magnetic field and baryochemical potential.

Acknowledgement

BS and KKP acknowledge the financial aid from CSIR and UGC, the Government of India, respectively. The authors gratefully acknowledge the DAE-DST, Government of India funding under the mega-science project "Indian Participation in the ALICE experiment at CERN" bearing Project No. SR/MF/PS-02/2021-IITI (E-37123). The authors would like to acknowledge some fruitful discussions with Girija Sankar Pradhan during the preparation of the manuscript.

-
- [1] S. Borsanyi, Z. Fodor, C. Hoelbling, S. D. Katz, S. Krieg and K. K. Szabo, Phys. Lett. B **730**, 99 (2014).
- [2] A. Bazavov *et al.* [HotQCD], Phys. Rev. D **90**, 094503 (2014).
- [3] R. Bellwied, S. Borsanyi, Z. Fodor, S. D. Katz and C. Ratti, Phys. Rev. Lett. **111**, 202302 (2013).
- [4] A. Bazavov *et al.* [HotQCD], Phys. Rev. D **86**, 034509 (2012).
- [5] R. Bellwied, S. Borsanyi, Z. Fodor, J. Gunther, K. H. Kampert, S. D. Katz, T. Kawanai, T. G. Kovacs, S. W. Mages and A. Pasztor, *et al.* Nucl. Phys. A **967**, 732 (2017).
- [6] S. Borsanyi, G. Endrodi, Z. Fodor, A. Jakovac, S. D. Katz, S. Krieg, C. Ratti and K. K. Szabo, JHEP **11**, 077 (2010).
- [7] F. Karsch, K. Redlich and A. Tawfik, Eur. Phys. J. C **29**, 549 (2003).
- [8] P. Huovinen and P. Petreczky, Nucl. Phys. A **837**, 26 (2010).
- [9] F. Karsch, K. Redlich and A. Tawfik, Phys. Lett. B **571**, 67 (2003).
- [10] A. Tawfik, Phys. Rev. D **71**, 054502 (2005).
- [11] C. R. Allton, M. Doring, S. Ejiri, S. J. Hands, O. Kaczmarek, F. Karsch, E. Laermann and K. Redlich, Phys. Rev. D **71**, 054508 (2005).
- [12] S. Borsanyi, G. Endrodi, Z. Fodor, S. D. Katz, S. Krieg, C. Ratti and K. K. Szabo, JHEP **08**, 053 (2012).
- [13] P. Braun-Munzinger, K. Redlich, and J. Stachel, in Quark Gluon Plasma 3, edited by R. C. Hwa and X. N. Wang (World Scientific, Singapore, 2004).
- [14] R. Dashen, S. K. Ma and H. J. Bernstein, Phys. Rev. **187**, 345 (1969).
- [15] R. Venugopalan and M. Prakash, Nucl. Phys. A **546**, 718 (1992).
- [16] A. Bhattacharyya, S. K. Ghosh, R. Ray and S. Samanta, EPL **115**, 62003 (2016).
- [17] R. Hagedorn and J. Rafelski, Phys. Lett. B **97**, 136 (1980).
- [18] D. H. Rischke, M. I. Gorenstein, H. Stoecker and W. Greiner, Z. Phys. C **51**, 485 (1991).

- [19] J. Cleymans, M. I. Gorenstein, J. Stalnacke and E. Suonen, *Phys. Scripta* **48**, 277 (1993).
- [20] G. D. Yen, M. I. Gorenstein, W. Greiner and S. N. Yang, *Phys. Rev. C* **56**, 2210 (1997).
- [21] J. Fu, *Phys. Rev. C* **85**, 064905 (2012).
- [22] J. Fu, *Phys. Lett. B* **722**, 144 (2013).
- [23] A. Andronic, P. Braun-Munzinger, J. Stachel and M. Winn, *Phys. Lett. B* **718**, 80 (2012).
- [24] C. P. Singh, B. K. Patra and K. K. Singh, *Phys. Lett. B* **387**, 680 (1996).
- [25] M. I. Gorenstein, M. Hauer and O. N. Moroz, *Phys. Rev. C* **77**, 024911 (2008).
- [26] A. Tawfik, *Phys. Rev. C* **88**, 035203 (2013).
- [27] V. V. Begun, M. Gazdzicki and M. I. Gorenstein, *Phys. Rev. C* **88**, 024902 (2013).
- [28] A. Bhattacharyya, S. Das, S. K. Ghosh, R. Ray and S. Samanta, *Phys. Rev. C* **90**, 034909 (2014).
- [29] K. A. Bugaev, M. I. Gorenstein, H. Stoecker and W. Greiner, *Phys. Lett. B* **485**, 121 (2000).
- [30] V. V. Sagun, A. I. Ivanytskyi, K. A. Bugaev and I. N. Mishustin, *Nucl. Phys. A* **924**, 24 (2014).
- [31] S. Pal, G. Kadam and A. Bhattacharyya, *Nucl. Phys. A* **1023**, 122464 (2022).
- [32] G. Kadam and H. Mishra, *Phys. Rev. D* **100**, 074015 (2019).
- [33] D. Anchishkin and V. Vovchenko, *J. Phys. G* **42**, 105102 (2015).
- [34] S. Pal, A. Bhattacharyya and R. Ray, *Nucl. Phys. A* **1010**, 122177 (2021).
- [35] H. X. Zhang, J. W. Kang and B. W. Zhang, *Phys. Rev. D* **101**, 114033 (2020).
- [36] S. Samanta and B. Mohanty, *Phys. Rev. C* **97**, 015201 (2018).
- [37] V. Vovchenko, D. V. Anchishkin and M. I. Gorenstein, *Phys. Rev. C* **91**, 064314 (2015).
- [38] V. Vovchenko, M. I. Gorenstein and H. Stoecker, *Phys. Rev. Lett.* **118**, 182301 (2017).
- [39] N. Sarkar and P. Ghosh, *Phys. Rev. C* **98**, 014907 (2018).
- [40] K. K. Pradhan, D. Sahu, R. Scaria and R. Sahoo, *Phys. Rev. C* **107**, 014910 (2023).
- [41] V. Skokov, A. Y. Illarionov and V. Toneev, *Int. J. Mod. Phys. A* **24**, 5925 (2009).
- [42] A. N. Tawfik, A. M. Diab, N. Ezzelarab and A. G. Shalaby, *Adv. High Energy Phys.* **2016**, 1381479 (2016).
- [43] A. Bzdak and V. Skokov, *Phys. Lett. B* **710**, 171 (2012).
- [44] W. T. Deng and X. G. Huang, *Phys. Rev. C* **85**, 044907 (2012).
- [45] R. C. Duncan and C. Thompson, *Astrophys. J. Lett.* **392**, L9 (1992).
- [46] P. Dey, A. Bhattacharyya and D. Bandyopadhyay, *J. Phys. G* **28**, 2179 (2002).
- [47] T. Vachaspati, *Phys. Lett. B* **265**, 258 (1991).
- [48] J. R. Bhatt and A. K. Pandey, *Phys. Rev. D* **94**, 043536 (2016).
- [49] D. E. Kharzeev, L. D. McLerran and H. J. Warringa, *Nucl. Phys. A* **803**, 227 (2008).
- [50] K. Fukushima, D. E. Kharzeev and H. J. Warringa, *Phys. Rev. D* **78**, 074033 (2008).
- [51] G. S. Bali, F. Bruckmann, G. Endrodi, Z. Fodor, S. D. Katz, S. Krieg, A. Schafer and K. K. Szabo, *JHEP* **02**, 044 (2012).
- [52] I. A. Shovkovy, *Lect. Notes Phys.* **871** 13 (2013).
- [53] F. Preis, A. Rebhan and A. Schmitt, *JHEP* **03**, 033 (2011).
- [54] F. Bruckmann, G. Endrodi and T. G. Kovacs, *JHEP* **04**, 112 (2013).
- [55] G. S. Bali, F. Bruckmann, M. Constantinou, M. Costa, G. Endrodi, S. D. Katz, H. Panagopoulos and A. Schafer, *Phys. Rev. D* **86**, 094512 (2012).
- [56] G. S. Bali, G. Endrödi, and S. Piemonte, *JHEP* **07**, 183 (2020).
- [57] F. Lin, K. Xu and M. Huang, *Phys. Rev. D* **106**, 016005 (2022).
- [58] K. Xu, J. Chao and M. Huang, *Phys. Rev. D* **103**, 076015 (2021).
- [59] C. Bonati, M. D'Elia, M. Mariti, F. Negro and F. Sanfilippo, *Phys. Rev. D* **89**, 054506 (2014).
- [60] C. Bonati, M. D'Elia, M. Mariti, F. Negro and F. Sanfilippo, *Phys. Rev. Lett.* **111**, 182001 (2013).
- [61] G. S. Bali, F. Bruckmann, G. Endrödi, S. D. Katz and A. Schäfer, *JHEP* **08**, 177 (2014).
- [62] N. Chaudhuri, S. Ghosh, P. Roy and S. Sarkar, *Phys. Rev. D* **106**, 056020 (2022).
- [63] A. N. Tawfik, A. M. Diab and M. T. Hussein, *J. Phys. G* **45**, 055008 (2018).
- [64] G. Endrödi, *JHEP* **04**, 023 (2013).
- [65] G. Kadam, S. Pal and A. Bhattacharyya, *J. Phys. G* **47**, 125106 (2020).
- [66] G. S. Pradhan, D. Sahu, S. Deb and R. Sahoo, *J. Phys. G* **50**, 055104 (2023).
- [67] L. Landau and E. Lifshits, *Quantum mechanics: non-relativistic theory*, Course of theoretical physics volume 3, Pergamon Press, U.K. (1977).
- [68] S. Chakrabarty, *Phys. Rev. D* **54**, 1306 (1996).
- [69] E. S. Fraga and A. J. Mizher, *Phys. Rev. D* **78**, 025016 (2008).
- [70] C. Kittel, *Elementary statistical physics*, Dover Books on Physics Series, Dover Publications, U.S.A. (2004).
- [71] H. Stanley, *Introduction to phase transitions and critical phenomena*, The International Series of Monographs on Physics Series, Oxford University Press, Oxford U.K. (1987).
- [72] V. Vovchenko, D. V. Anchishkin, M. I. Gorenstein and R. V. Poberezhnyuk, *Phys. Rev. C* **92**, 054901 (2015).
- [73] D. P. Menezes, M. Benghi Pinto, S. S. Avancini, A. Perez Martinez and C. Providencia, *Phys. Rev. C* **79**, 035807 (2009).
- [74] M. Peskin and D. Schroeder, *An introduction to quantum field theory*, Westview Press, U.S.A. (1995).
- [75] Ramond P 2001 *Field Theory: A Modern Primer* (CO, USA: Westview Press)
- [76] Digital library of mathematical functions, release date 2012-03-23, National Institute of Standards and Technology, <http://dlmf.nist.gov/>.
- [77] Elizalde E 1986 An asymptotic expansion for the first derivative of the generalized Riemann zeta function *Math. Comp.* **47** 347.
- [78] C. Patrignani *et al.* (Particle Data Group), *Chin. Phys. C* **40**, 100001 (2016).
- [79] Griffiths, David J. (David Jeffery), 1942-. *Introduction to Electrodynamics*. Boston :Pearson, 2013.
- [80] J. S. Schwinger, *Phys. Rev.* **82**, 664 (1951).
- [81] P. Elmfors, D. Persson and B. S. Skagerstam, *Astropart. Phys.* **2**, 299 (1994).
- [82] J. O. Andersen and R. Khan, *Phys. Rev. D* **85**, 065026 (2012).
- [83] N. A. Tawfik, L. I. Abou-Salem, A. G. Shalaby, M. Hanafy, A. Sorin, O. Rogachevsky and W. Scheinast,

Eur. Phys. J. A **52**, 324 (2016).

- [84] P. Braun-Munzinger, D. Magestro, K. Redlich, and J. Stachel, Phys. Lett. B 518, 41 (2001).
 [85] J. Cleymans, H. Oeschler, K. Redlich, and S. Wheaton, Phys. Rev. C 73, 034905 (2006).
 [86] A. Khuntia, S. K. Tiwari, P. Sharma, R. Sahoo, and T. K. Nayak, Phys. Rev. C 100, 014910 (2019).
 [87] J. Liu, M. j. Luo, Q. Wang and H. j. Xu, Phys. Rev. D **84**, 125027 (2011).
 [88] J. Liu, M. j. Luo, and H. j. Xu, Cent. Eur. J. Phys. **10**, 1369 (2012).

Appendix A: Squared speed of sound

The squared speed of sound is given by,

$$c_s^2(T, \mu, QB) = \left(\frac{\partial P}{\partial \epsilon} \right)_{s/n}. \quad (\text{A1})$$

Using the variables T , μ and QB this can be rewritten as

$$c_s^2(T, \mu, QB) = \frac{dP}{d\epsilon} = \frac{\frac{\partial P}{\partial T} + \frac{\partial P}{\partial \mu} \frac{d\mu}{dT} + \frac{\partial P}{\partial(QB)} \frac{d(QB)}{dT}}{\frac{\partial \epsilon}{\partial T} + \frac{\partial \epsilon}{\partial \mu} \frac{d\mu}{dT} + \frac{\partial \epsilon}{\partial(QB)} \frac{d(QB)}{dT}} \quad (\text{A2})$$

Number density (n) and entropy (s) of a system is a function of (T, μ, QB) The first condition is keeping the ratio (s/n) constant. From the derivative, one obtains

$$d\left(\frac{s}{n}\right) = 0, \quad (\text{A3})$$

which implies

$$nds = sdn. \quad (\text{A4})$$

Divide both sides by dT so that the above Eq. (??) can be modified as,

$$n\left(\frac{ds}{dT}\right) = s\left(\frac{dn}{dT}\right). \quad (\text{A5})$$

One can write $n(T, \mu, QB)$ and $s(T, \mu, QB)$ in the form of differential as,

$$dn = \frac{\partial n}{\partial T} dT + \frac{\partial n}{\partial \mu} d\mu + \frac{\partial n}{\partial(QB)} d(QB) \quad (\text{A6})$$

So if we divide both sides of the Eq. (A6) by dT , then we have,

$$\frac{dn}{dT} = \frac{\partial n}{\partial T} + \frac{\partial n}{\partial \mu} \frac{d\mu}{dT} + \frac{\partial n}{\partial(QB)} \frac{d(QB)}{dT} \quad (\text{A7})$$

Similarly for $s(T, \mu, QB)$ we can write,

$$ds = \frac{\partial s}{\partial T} dT + \frac{\partial s}{\partial \mu} d\mu + \frac{\partial s}{\partial(QB)} d(QB) \quad (\text{A8})$$

$$\frac{ds}{dT} = \frac{\partial s}{\partial T} + \frac{\partial s}{\partial \mu} \frac{d\mu}{dT} + \frac{\partial s}{\partial(QB)} \frac{d(QB)}{dT} \quad (\text{A9})$$

Substituting Eq. (A7) and Eq. (A9) in Eq. (A5) we get,

$$n\left(\frac{\partial s}{\partial T} + \frac{\partial s}{\partial \mu} \frac{d\mu}{dT} + \frac{\partial s}{\partial(QB)} \frac{d(QB)}{dT}\right) = s\left(\frac{\partial n}{\partial T} + \frac{\partial n}{\partial \mu} \frac{d\mu}{dT} + \frac{\partial n}{\partial(QB)} \frac{d(QB)}{dT}\right). \quad (\text{A10})$$

$$\begin{aligned} \frac{d\mu}{dT} \left(n \frac{\partial s}{\partial \mu} - s \frac{\partial n}{\partial \mu} \right) &= s \left(\frac{\partial n}{\partial T} + \frac{\partial n}{\partial(QB)} \frac{d(QB)}{dT} \right) - n \left(\frac{\partial s}{\partial T} + \frac{\partial s}{\partial(QB)} \frac{d(QB)}{dT} \right) \\ &\Rightarrow \frac{d\mu}{dT} = \frac{\left(s \frac{\partial n}{\partial T} - n \frac{\partial s}{\partial T} \right) + \left(s \frac{\partial n}{\partial(QB)} - n \frac{\partial s}{\partial(QB)} \right) \frac{d(QB)}{dT}}{n \frac{\partial s}{\partial \mu} - s \frac{\partial n}{\partial \mu}} \end{aligned} \quad (\text{A11})$$

Similarly, one can evaluate $\frac{d(QB)}{dT}$ from Eq. (A10) as follows,

$$\frac{d(QB)}{dT} = \frac{\left(s \frac{\partial n}{\partial T} - n \frac{\partial s}{\partial T} \right) + \left(s \frac{\partial n}{\partial \mu} - n \frac{\partial s}{\partial \mu} \right) \frac{d\mu}{dT}}{n \frac{\partial s}{\partial(QB)} - s \frac{\partial n}{\partial(QB)}} \quad (\text{A12})$$

For a finite baryon chemical potential and finite external magnetic field, the above two transcendental equations can be solved numerically to find the speed of sound of the system.

Appendix B: Magnetic susceptibility (χ_M^2)

In this paper, the magnetic susceptibility is calculated using Eq. (27),

$$\chi_{M,i}^2 = \frac{\pm g_i}{2\pi^2} \int_0^\infty dp_z \left[Q_i B \left(- \frac{(k + \frac{1}{2} - s_z)^2}{(E^z)^2 T [\exp(\frac{E_i^z - \mu_i}{T}) \pm 1]^2} \pm \frac{(k + \frac{1}{2} - s_z)^2}{(E^z)^2 T [\exp(\frac{E_i^z - \mu_i}{T}) \pm 1]} \pm \frac{(k + \frac{1}{2} - s_z)^2}{(E^z)^{3/2} [\exp(\frac{E_i^z - \mu_i}{T}) \pm 1]} \right) \mp \frac{2(k + \frac{1}{2} - s_z)}{E^z [\exp(\frac{E_i^z - \mu_i}{T}) \pm 1]} \right]. \quad (\text{B1})$$

Appendix C: Electrical susceptibility (χ_Q^2)

The electrical susceptibility is calculated using Eq. (29),

$$\chi_{Q,i}^2 = \frac{g_i Q_i^3 B}{2\pi^2 T^3} \int_0^\infty dp_z \frac{\exp(\frac{E_i^z - \mu_i}{T})}{[\exp(\frac{E_i^z - \mu_i}{T}) \pm 1]^2}. \quad (\text{C1})$$

Appendix D: Vacuum contribution for Magnetization (ΔM)

The explicit form of vacuum contribution for magnetization is obtained using Eq. (69). For spin-0 particles,

$$\Delta \mathcal{M}_{vac}^r(S=0, B) = \frac{\partial(\Delta P_{vac}(S=0, B))}{\partial(eB)}. \quad (\text{D1})$$

On simplifying,

$$\Delta \mathcal{M}_{vac}^r(S=0, B) = \frac{|Q|B}{8\pi^2} \left[\frac{x}{12(x+1/2)} + x^2 \ln(x+1/2) - \frac{(x+1/2)^{-2}}{360} \left(\frac{x}{x+1/2} - 1 \right) - \frac{(1+\ln x)}{12} - 2 \left(\frac{1}{12} - \frac{x+1/2}{2} + \frac{(x+1/2)^2}{2} \right) \ln(x+1/2) \right]. \quad (\text{D2})$$

For spin-1/2 particles,

$$\Delta \mathcal{M}_{vac}^r(S=1/2, B) = \frac{\partial(\Delta P_{vac}(S=1/2, B))}{\partial(eB)}, \quad (\text{D3})$$

$$\Delta \mathcal{M}_{vac}^r(S=1/2, B) = \frac{-|Q|B}{720\pi^2 x^2}. \quad (\text{D4})$$

Similarly, for spin-1 particles one can write,

$$\Delta \mathcal{M}_{vac}^r(S=1, B) = \frac{\partial(\Delta P_{vac}(S=1, B))}{\partial(eB)}, \quad (\text{D5})$$

$$\Delta \mathcal{M}_{vac}^r(S=1, B) = \frac{3|Q|B}{8\pi^2} \left[\frac{x}{12(x-1/2)} + x^2 \ln(x-1/2) - \frac{(x-1/2)^{-2}}{360} \left(\frac{x}{x-1/2} - 1 \right) - 2 \left(\frac{1}{12} - \frac{x-1/2}{2} + \frac{(x-1/2)^2}{2} \right) \ln(x-1/2) - \frac{(x+1)\ln(x+1/2)}{3} + \frac{(2-5x)\ln(x-1/2)}{3} + \frac{(3+7\ln x)}{12} \right], \quad (\text{D6})$$

where, $x = \frac{m^2}{2|Q|B}$. Now, the total vacuum contribution consists of the contribution from the spin-0, spin-1/2 and spin-1 particles. So, we finally get,

$$\Delta\mathcal{M}_{vac}^r = \Delta\mathcal{M}_{vac}^r(S = 0, B) + \Delta\mathcal{M}_{vac}^r(S = 1/2, B) + \Delta\mathcal{M}_{vac}^r(S = 1, B). \quad (\text{D7})$$
